Indian Journal of Chemistry
Vol. 63, December 2024, pp. 1183-1191
DOI: 10.56042/ijc.v63i12.6896

Influence of intramolecular ring-ring π,π-interaction on crystal building in ternary compound of nickel(II) chelates of 2,2'-{[2-(4-methylphenyl)ethyl]azanediyl} diacetic acid and 1,10-phenanthroline – Synthesis, spectral, optical and quantum chemical study

Dheerendra Kumar Patel*[a†], Duane Choquesillo-Lazarte[b], Josefa María González-Pérez[a] & Juan Niclós-Gutiérrez[a]

[a] Department of Inorganic Chemistry, Faculty of Pharmacy, University of Granada, E-18071 Granada, Spain

[b] Laboratorio de EstudiosCristalográficos, IACT-CSIC Avda. de las Palmeras 4, 18100 Armilla, Spain

E-mail: dkprewa@yahoo.co.in

Received 23 November 2023; accepted(revised) 22 March 2024

The stoichiometric reaction between Ni(II) hydroxy-carbonate and N-(*p*-methyl-phenethyl)-Iminodiacetic acid ligand (H_2MEpheida) in aqueous media leads to binary complex of the type [Ni(MEpheida)(H_2O)$_3$]·xH_2O which gives ternary complex of the formula [Ni(MEpheida)(phen)(H_2O)]·3H_2O on the addition of 1,10-phenanthroline (1,10-phen) in equimolar ratio. The compound has been characterized by means of elemental analysis, FTIR, UV-Vis, TGA and X-ray crystallography. The weak ring-ring intramolecular π,π-interaction between phen and benzene ring of MEpheida affects the crystal pattern of the complex (triclinic, space group P-1) reported herein. Crystallographic information reveals the distorted octahedral geometry of the type 1+2+2+1 (lesser Jahn-Teller distortion) around the Ni(II) ion with full and half occupancy of t_{2g}^6 and $3dx^2$-y^2, $3dz^2$ orbitals respectively. The iminodiacetate moiety of metal-chelate adopts *fac*-NO_2 conformation. Moreover, the quantum chemical calculations and HOMO-LUMO energy gap along with the other global descriptors have been performed for the H_2MEpheida and [Ni(MEpheida)(phen)(H_2O)] complex using DFT/B3LYP methodology. The optical bandgap energy (E_g) for ligand and Ni(II) complex have been estimated through Tauc's equation, $\alpha h\nu = A(h\nu - E_g)^r$, where r = ½ for indirect and 2 for direct electronic transitions using electronic absorption data. The direct and indirect electronic transition bandgap calculated for Ni(II) complex 3.97 and 3.76 eV respectively, reflecting their semi-conducting nature.

Keywords: Nickel(II) ternary complex, Molecular structure, Supra-molecular chemistry, HOMO-LUMO calculations, Optical bandgap energy measurements

The ternary metal complexes of copper(II) with iminodiacetic acid (H_2IDA) and/or derivative of iminodiacetic acid (H_2IDA-like) ligands have been extensively studied since last three decades owing to their flexible coordination geometry surrounding the copper(II) ion and conformational versatility of the chelating ligands. The flexible conformational mode of IDA and IDA-like chelating ligands (facial and/or meridional) of the type *mer*-NO_2 and/or *fac*-NO+O (apical/distal), *fac*–O_2+N (apical/distal)play an important role in their catalytic and antimicrobial properties[1]. The IDA-derivative ligands of the type N-(*R*)-IDA where R = benzyl-, *para*-substituted benzyl-, phenethyl- and *para*-substituted phenethyl- substrate are enabling the possibilities of π···π and C-H···π-intra and inter-molecular interactions[2,3]. These inter and intra-molecular weak interactions play an important role in molecular recognitions, supramolecular behaviour and crystal building. The role of these non-coordinating moiety of the N-(*R*)-IDA-like ligands have been revealed from the structures obtained from the CSD database. In this context, our group reported a tetranuclear complex, Cu(II)-(pheida) chelate (pheida = Ph-CH_2-CH_2-N(CH_2-COO^-)$_2$) with bridging mode of adenine μ_2-N_3,N_7-(H9)ade and a bis-chelate salt having formula [Cu(phen)$_3$][Cu(pheida)$_2$]. In addition to this, a ternary molecular complex of the type [Cu(pheida)(Hhyp)(H_2O)]·2H_2O (Hhyp = hypoxanthine) also have been reported recently[4]. Moreover, recently we have reported some binary molecular complexes of the type [M(MOpheida)(H_2O)$_3$] (M = Ni(II), Co(II)),

† Present Address: Department of Chemistry, Governmentt SGS Post Graduate College, Ganj Basoda 464 221 [Affiliated to Barkatullah University, Bhopal (MP) India].

[Ni(Fpheida)$(H_2O)_3$] and [Co(pheida)$(H_2O)_3$]·1.5H_2O where MOpheida = N-(*p*-methoxy)-phenethyl-iminodiacetate(2–) and Fpheida = N-(*p*-fluro)-phenethyl-iminodiacetate(2-) respectively[5]. The presence of *cis*-diaqua ligands in these latter reported octahedral complexes enable them to produce variety of mixed-ligand complexes with imidazoles, α,α′-diimines (2,2-bipyrine, 1,10-phenanthroline) and other mono or bi-dentate ligands. In this context, we report a complex of the formula [Ni(MEpheida)(phen)(H_2O)]·3H_2O where MEpheida = N-(*p*-methyl-phenethyl)-iminodiacetate (2-) chelating ligand and phen = 1,10-phenanthroline.

There are two main objectives of this work, first is to look into the effect of weak ring-ring, π···π intramolecular interaction in crystal building and second is to measure the semi-conducting nature and quantum chemical study of ligand and their nickel(II) ternary complex reported herein.

Experimental Section

Chelating ligand and other materials

The basic nickel carbonate [$NiCO_3$·2Ni$(OH)_2$·4H_2O] for the source of nickel(II) ion was purchased from Merck and used as received. The tridentate chelating ligand H_2MEpheida acid was prepared according to previously reported ligand, N(phenethyl)-iminodiacetic acid (H_2pheida)[6], but using *p*-methyl-phenethylamine in place of *N*-phenethylamine. The H_2MEpheida acid was prepared in our laboratory using *p*-methyl-phenethylamine (CH_3-C_6H_4-CH_2-CH_2-NH_2) and potassium chloroacetate (Cl-CH_2-COOK) (both purchased from Aldrich) in 1:2 ratio, respectively. The alkaline aqueous solution (*p*H ~ 11) was stirred well at 90°C, for approximately 2.5 h, then reaction mixture was allowed to cool up to ~10°C temperature and acidified with hydrochloric acid 6N (*p*H ~ 3-2.5) until desired acid product precipitated and collected by filtration. Further addition of 6N, hydrochloric acid produce fraction of ligand, and washed with distilled water. The white crystalline product reacted with $NaHCO_3$ in distilled water until clear solution formed and re-crystallized by the addition of an equivalent amount of 6N, HCl. The recrystallized H_2MEpheida ligand washed with water and air dried (Scheme 1). Various attempts failed to grow suitable crystal for single crystal X-ray. For (H_2MEpheida) starting from 0.5 mol of *p*-methyl-phenethylamine, the yield was 196 g, 78%. *Anal.* Calc. for $C_{13}H_{17}NO_4$(%): C, 62.14; H, 6.82; N, 5.57. Found: C, 62.10; H, 6.85; N, 5.61%. The relevant FT-IR frequencies (cm^{-1}): three easily distinguishable peaks 3020, 2962 and 2915 can be assigned to $\nu_{(C\text{-}H)}$ modes; for peaks at 2700-2300, including one at 2570 for $\nu_{(N^+\text{–}H)}$. Moreover, 3452m (broad), peaks at 1720, 1248 and 710 can be assigned for $\nu_{(O\text{-}H)}$, $\nu_{(C=O)}$, $\delta_{(O\text{-}H)}$ and $\pi_{(O\text{-}H)}$ of free acid –COOH group; 1618 and 1384 for ν_{as} and ν_s of carboxylate ion (COO^-).

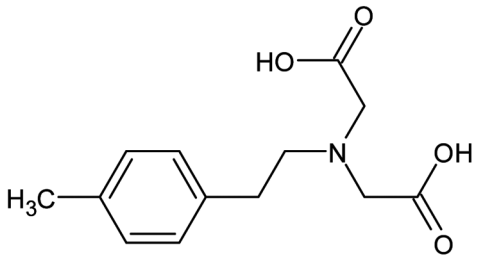

Scheme 1 — Structure of chelating ligand, 2,2'-{[2-(4-methylphenyl)ethyl] azanediyl} diacetic acid

Synthesis of nickel(II) complex

The ternary complex of nickel(II) was obtained through the stoichiometric reaction between nickel(II) basic carbonate [$NiCO_3$·2Ni$(OH)_2$·4H_2O], (124 mg, 0.33 mmol Ni ≥ 47%) and H_2MEpheida (251 mg, 1 mmol) in 150 mL distilled water in a Kitasato flask by heating at 70°C under reduced pressure (to remove the CO_2, a by-product of the reaction) for 3 hours, until greenish solution seems to be obtained. The solution was slowly filtered without vacuum in another Kitasato flask through a sintered disk filter funnel (Ø 10-16 μm) to remove very small amount of unreacted nickel oxide. After that, in the same solution 1,10-phen (180 mg, 1 mmol, Merck ≥ 99%) was added and stirred well at RT until desired intense blue-green clear solution observed. The solution was filtered in a crystallization device, covered with plastic and left for slow evaporation at RT. After 3-4 weeks, well-shaped dark blue-green crystals appeared which were suitable for X-ray diffraction. The fraction of crystals was obtained from the mother solution in similar ways. The product was washed with cool water and air-dried. The yield of the complex was more than 50%. *Anal.* Calc. for complex [Ni(MEpheida)(phen)(H_2O)]·3H_2O, ($C_{25}H_{31}N_3NiO_8$) (MW: 560.24) (%): C, 53.60; H, 5.58; N, 7.50; Ni, 10.48%. Found: C, 53.52; H, 5.59; N, 7.55; Ni, 10.42%.

Physical measurements

A Fisons-Carlo Erba EA 1108 elemental micro-analyzer was used for the elemental micro-analysis of

the ligands and nickel(II) complex. The vibrational spectra were recorded (KBr pellets, range 4000-400 cm^{-1}) with a Jasco FT-IR 410 spectrophotometer. A Varian Cary-5E spectrometer was used for obtaining the electronic absorption spectra. The pyrolytic TG analysis of the complex (295-800ºC) were performed in CO_2-free dry-air flow (100 mL min^{-1}) by a Shimadzu Thermobalance TGA–DTG–50H instrument, until a series of FT-IR spectra of gases were recorded (to identify the evolved gases) using a coupled FT-IR Nicolet Magma 550 spectrometer.

X-ray diffraction data collection and structural refinement

Suitable blue-green crystal mounted on glass fibre and the sample was used for data collection and summarized in Table 1. Data were collected with Bruker X8 Proteum (*T = 293 K*) diffractometer. The data were processed with APEXII[7] and corrected for absorption using SADABS[8]. The structure solved by direct method[9], which revealed the position of all non-hydrogen atoms. These atoms were refined on F^2 by a full-matrix least-squares procedure using anisotropic displacement parameters[10]. All hydrogen atoms were located in difference Fourier maps and included as fixed contributions riding on attached atoms with isotropic thermal displacement parameters 1.2 times than those of the respective atom. Geometric calculations were carried out with PLATON[11] and drawings were produced with PLATON[11] and MERCURY[12]. The bond lengths of atoms directly attached to the nickel(II) and bond angles are given in Table 2.

Quantum Chemical Calculations

The quantum chemical calculations were carried out for ligand and their nickel(II) ternary complex using Avogadro (a molecular builder and visualizer) and Orca programs[13] and the obtained results were compared with crystallographic and other spectral experimental data. The Becke's three parameter exchange functional[14,15] and Lee-Yang-Par non-local correlation functional (B3LYP)[16]with the aid of orbital basis set def2-SVP or def2-TZVP (for Ni(II) complex) were utilized for computational calculations. The single point energy (SPE) of the H_2MEpheida and nickel(II) complex have been measured in various level of theory and results were listed in Table 3, using restricted Hartree-Fock, RHF/MP2/DFT and unrestricted Hartree-Fock, UHF/MP2/DFT methods, respectively. Along with

Table 1 — Details of crystallographic data collection and structural refinement for Ni(II) complex.

Compd	[Ni(MEpheida)(phen)(H_2O)] $3H_2O$
Empirical formula	C_{25} H_{31} N_3 Ni O_8
Formula weight	560.24
Crystal system	Triclinic
Space group	P-1
Unit cell dimensions	
a (Å)	9.8693(5)
b (Å)	11.4745(6)
c (Å)	12.6233(6)
α (º)	112.7580(10)
β (º)	93.195(2)
γ (º)	94.5030(10)
V ($Å^3$)	1308.39(11)
Z	2
Calculated density (mg m^{-3})	1.422
Absorption coefficient (mm^{-1})	1.525
F (000)	588
Crystal size (mm)	0.30×0.28×0.15
Θ Range data collected (º)	7.62 to 66.49
Refinement method	Full-matrix least-squares on F^2
Reflections collected/unique	4080 [*R*(int) = 0.0334]
Max/min transmission	0.8456 and 0.6024
Data/restraints/parameters	4080 / 0 / 335
Goodness-of-fit on F^2	1.090
Final *R* indices [I > 2σ(I)]	*R1 = 0.0381, wR2 = 0.1082*
R indices (all data)	*R1 = 0.0383, wR2 = 0.1083*
Type of crystal	Single crystal

Table 2 — X-ray and computational coordination bond lengths (Å) and *trans*-angles (°) for Ni(II) complex.

Coordination linkage	Bond length (Å)	
	X-ray	DFT
Ni(1)-N(1)(amine)	2.158(14)	2.153
Ni(1)-O(33)(aqua)	2.060(13)	2.068
Ni(1)-O(4)(carboxylato)	2.027(13)	2.029
Ni(1)-N(19)(imine)	2.103(15)	2.109
Ni(1)-N(30)(imine)	2.102(15)	2.107
Ni(1)-O(8)(carboxylato)	2.046(12)	2.042
Coordination linkage	*Trans*-angle (°)	
	X-ray	DFT
N(1)-Ni(1)-O(33)	166.56(6)	166.49
N(19)-Ni(1)-O(4)	172.65(6)	172.78
N(30)-Ni(1)-O(8)	168.75(6)	168.30

Table 3 — Calculated SPE (eV) of H_2MEpheida and their corresponding Ni(II) ternary complex at different levels of theory.

Theory level	H_2MEpheida	1,10-phen	Ni(II) complex
RHF/UHF	–855.4393	–567.5458	–3193.8397
MP2	–858.0740	–569.4056	–3201.4873
DFT	–860.6465	–571.1914	–3205.9108

the SPE, enthalpy change (ΔH), entropy change (ΔS) and Gibbs energy (ΔG) of the chelators and complex are also calculated at same level of theory. The analytical vibrational frequency calculations have been performed by using DFT with the aid of def2-SVP and def2/J basis sets after obtaining the optimized geometry of the compounds. The excited state electronic absorption spectra (TD-DFT) were obtained for the ligand and Ni(II) complex using B3LYP theory with the aid of def2-TZVP, def2/J and RIJCOSX functional. The optimized energy and energy gap (ΔE) of highest occupied molecular orbitals (HOMO) and lowest unoccupied molecular orbitals (LUMO) of frontier molecular orbitals (FMOs) are also obtained at same level of theory. Moreover, hardness (η, eV), softness (σ, eV^{-1}) and dipole moment (μ, D) of the H_2MEpheida and nickel(II) complex are also calculated from DFT calculations using the following equations[17]:

$$\eta = ½ (Ip\text{-}Ea) \quad \ldots(1)$$

$$\sigma = 1/\eta \quad \ldots(2)$$

where, *Ip* is ionization potential of the complex and *Ea* is electron affinity of the complex. *Ip* and *Ea* can be calculated using frontier molecular orbital (FMO) by applying Koopman's theorem[17].

$$Ip = -E \text{ (HOMO in eV)},$$
$$Ea = -E \text{ (LUMO in eV)} \quad \ldots(3)$$

$$\eta = -½ (E_{HOMO} - E_{LUMO}) = -\Delta E_{dif}/2 \quad \ldots(4)$$

where, ΔE = HOMO-LUMO energy difference.

Results and discussion

Molecular structure and supramolecular chemistry of Ni(II) ternary complex

The selected non-hydrogen bond lengths, *trans*-angles between L–M–L and hydrogen bonding distance and angles of the reported Ni(II) complex are given in Table 2. The nickel(II) complex consist of molecular unit along with three non-coordinated crystalline water molecule, [Ni(MEpheida)(phen)(H_2O)]·3H_2O (Fig. 1).

The compound crystallizes in the triclinic, space group P-1. The coordination polyhedron around the Ni(II) fulfilled by means of the atom N1(amino), O(4) and O(8) of (carboxylato; COO^-) preparing one face of the octahedron and supplied by chelating ligand. The two other coordination sites around the nickel(II) ion filled by imine (N19 and N30) nitrogen donor of 1,10-phen ligand, while, the sixth coordination cite is occupied by an aqua (O33, H_2O) ligand. The structural information reveals the distorted octahedral geometry of the type 1+2+2+1 (lesser Jahn-Teller distortion) around the Ni(II) ion where basal plane (2+2) built up by two oxygen atoms O(4) and O(8) and two imine nitrogen atoms N(19) and N(30) of H_2MEpheida and 1,10-phen ligand, respectively. The similar distorted octahedral coordination around the Ni(II) ion recognized as the most common geometry for the nickel(II) coordination compounds with variety of mono-, bi- and/or polydentate ligands. Notably, the *facial*-conformation (*fac*-NO_2) of IDA-moiety of H_2MEpheida ligand can be attributed to, not only the octahedral nickel(II) coordination environment, but also, for the rigid planarity of the 1,10-phenanthroline. Moreover, the crystallographic information reveals that the centrosymmetric unit cell consist of two asymmetric molecules (Fig. 2).

The molecules recognize to each other through ring-ring, π···π-stacking inter-molecular interaction between rings of 1,10-phen. The structural parameters for this π,π-stacking of the nickel(II) compound are: centroid (N19,C20,C21,C22,C23,C32)-centroid (N19,C20, C21, C22,C23, C32) distance for stacked six-membered rings d(C_I–C_J) = 5.322 Å; the dihedral angles between the I and J planes of the stacked rings α = 2.2°; β = 17.77° and γ = 19.15° (Fig. 3).

Moreover, intramolecular weak π,π-interaction is also observed between phenethyl ring of H_2MEphedia and imine ring of 1,10-phen: centroid-centroid

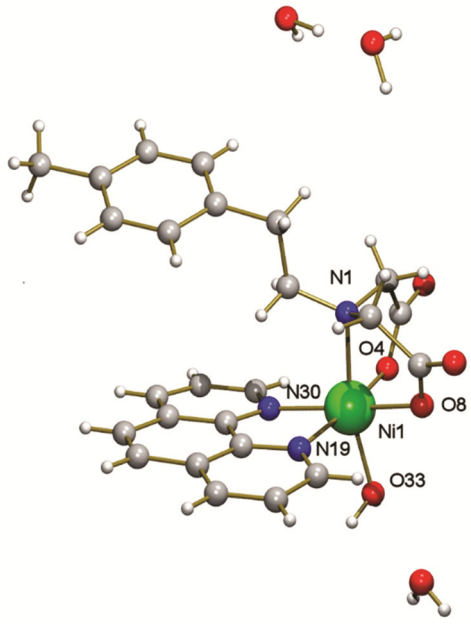

Fig. 1 — Structure of hydrated nickel(II) molecular complex with numbering of coordination linkage

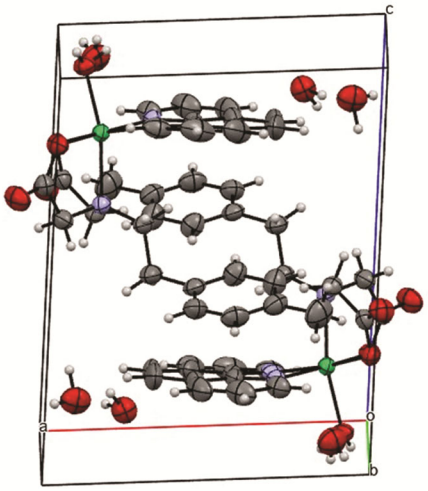

Fig. 2 — The ORTEP diagram exhibits two asymmetric molecules of Ni(II) complex in a centrosymmetric unit cell.

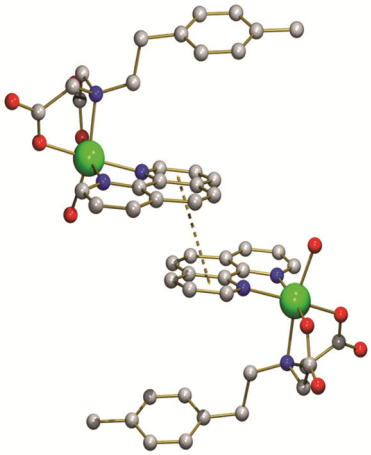

Fig. 3 — Centrosymmetric structure consisting of two asymmetric molecules recognize to each other through ring-ring, π···π-stacking inter-molecular interaction between rings of 1,10-phen.

distance for these stacked rings d(C_I–C_J) = 5.169 Å. In addition to these interactions, coordinated/non-coordinated (aqua/hydrate) O–H···O (non-coordinated water molecules) plus (aqua/hydrate) O-H···O (carboxylato, COO^-) of polar IDA arm are involved in molecular recognition forming 2D frameworks parallel to *ab* plane and hydrophobic MEpheida arm of chelating ligands oriented towards the external faces (Fig. 4, Table 4). Interestingly, the shortest intramolecular hydrogen bond observed for (aqua)O(33)–H(33B)···O(4)(COO^-) 1 2.685(18) Å, 164.7°; symmetry code 1 = –x, –y, –z. From the crystal data, Ni(1)–N(1) bond lengths is found highest with 2.159 Å, supplied by H_2MEpheida while lowest is observed for Ni(1)–O(4)(aqua) 2.027 Å. Moreover,

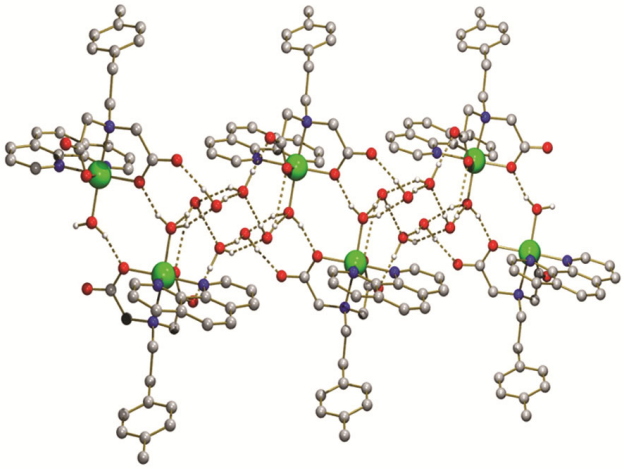

Fig. 4 — Showing 2D hydrogen-bonded chain (ribbon) that extends along the *b*-axis of the crystal and involves aqua ligands, carboxylate groups, and uncoordinated water molecules as donors/acceptors. The chains are connected by stacking interactions involving N30 rings of phenanthroline ligands of adjacent complex units, generating a 3D structure.

O(aqua) occupied *trans* coordination site to the N(IDA). The basal plane defining Ni–N/O bond lengths found 2.046-2.103 Å which are similar to the other reported nickel(II) octahedral complexes[18]. Notably, very close bond lengths 2.102-2.103 Å are observed for Ni(1)–N(19/30) *cis*-N(imine) donors supplied by rigid and planar 1,10-phen ligand. Additionally, in coordination polyhedra, the highest *trans*-angle observed for O(4)–Ni(1)–N(19) 172.65(6)° while, lowest found for N(1)–Ni(1)–(O33) 166.56(6)°.

Computational calculations

Single Point Energy (SPE)Measurements

The single point energy (SPE) of the chelating ligand, 1,10-phen and nickel(II) complex have been measured and results were summarized in Table 3 using restricted Hartree-Fock, RHF/MP2/DFT and unrestricted Hartree-Fock, UHF/MP2/DFT methods, respectively. The single point energy values are very close for each level of theory and the lowest data received form DFT measurements. Moreover, the lowest SPE observed for nickel(II) complex which reflect their higher stability can be attributed to the greater delocalization of electrons. The order of SPE found 1,10-phen > H_2MEpheida >Ni(II) complex.

ΔE measurements of FMOs

The energy difference (ΔE) of frontier molecular orbitals (FMOs) *i.e.*, highest occupied molecular

Table 4 — Bond lengths (Å) and angles of intra and inter-molecular hydrogen bonding interactions in Ni(II) complex

D–H···A	d(D–H)	d(H···A)	d(D···A)	<(DHA)	D–H···A	d(D–H)
O(33) –H(33B) ···O(4)#1	0.90	1.81	2.6845(2)	164.7	O(33) –H(33B) ···O(4)#1	0.90
O(33) –H(33A) ···O(3)#2	0.89	1.90	2.763(2)	162.6	O(33) –H(33A) ···O(3)#2	0.89
O(1) –H(1B)···O(2)#3	0.72	2.22	2.855(3)	147.0	O(1) –H(1B) ···O(2)#3	0.72
O(1) –H(1A) ···O(9)#3	1.01	1.74	2.739(2)	172.2	O(1) –H(1A) ···O(9)#3	1.01
O(2) –H(2A)···O(1)#4	0.81	2.06	2.877(3)	174.7	O(2) –H(2A) ···O(1)#4	0.81
O(2) –H(2B) ···O(33)#5	0.79	2.30	2.994(2)	147.7	O(2) –H(2B) ···O(33)#5	0.79
O(3) –H(3A) ···O(1)#6	0.98	1.80	2.767(2)	170.2	O(3) –H(3A) ···O(1)#6	0.98
O(3) –H(3B) ···O(5)#7	0.96	1.81	2.773(2)	174.9	O(3) –H(3B) ···O(5)#7	0.96

Symmetry transformations used to generate equivalent atoms: #1 –x,–y,–z #2 x,y,z–1 #3 x+1,y,z #4 –x+1,–y+1,–z , 5 –x,–y+1,–z #6 –x+1,–y+1,–z+1 #7 –x,–y,–z+1.

Table 5 — The quantum chemical calculations for the energy difference (ΔE_{dif}) of HOMO LUMO of ligands and Ni(II) complex using Koopman's theorem.

MO orbitals	FMOs energy (eV)			ΔH_{dif}(eV)		
	H_2MEpheida	1,10-phen	Ni(II) complex	H_2MEpheida	1,10-phen	Ni(II) complex
HOMO	–8.434	–8.624	–9.353	4.767	6.48	8.77
LUMO	3.667	2.144	0.583			
HOMO-1	–8.934	–10.244	–9.696	5.078	7.218	9.113
LUMO+1	3.856	3.026	0.583			
HOMO–2	–9.231	–10.358	–9.954	4.89	6.71	7.716
LUMO+2	4.341	3.648	2.238			
HOMO–3	–11.050	–10.848	–10.420	6.525	5.985	7.138
LUMO+3	4.525	4.863	3.282			
HOMO–4	–11.394	–10.856	–10.689	6.685	6.818	6.818
LUMO+4	4.709	4.899	3.871			

orbitals (HOMO) and lowest unoccupied molecular orbitals (LUMO) of ligands and their corresponding Ni(II) octahedral complex were optimized using DFT/B3LYP level of theory with the aid of def2-SVP (ligands) or def2-TZVP (for complex) orbital basis sets[19]. The results of these FMOs summarized in Table 5 and correlated with X-ray and other physico-chemical experimental data. Moreover, these data were also used for calculation of other global descriptors. Moreover, FMOs data also used to calculate the values of global descriptors such as hardness (η), softness (σ), dipole-moment (μ) which are generally utilized to assign the stability and chemical reactivity of the compounds. In all cases *i.e.*, H_2MEpheida, 1,10-phen and Ni(II) complex, the energy of LUMO orbitals are higher than corresponding HOMO orbitals. The higher HOMO-LUMO energy difference (ΔH_{dif}) calculated for Ni(II) complex(8.77 eV) than that of chelating (4.767 eV) and auxiliary ligand (6.48 eV) reflecting their higher kinetic stability with regard of chemical transformations (Fig. 5). Moreover, the highest ionization potential observed for nickel(II) complex (*Ip*, 9.353 eV) while lowest for H_2MEpheida (IP, 8.434 eV). In contrast, the highest electron affinity

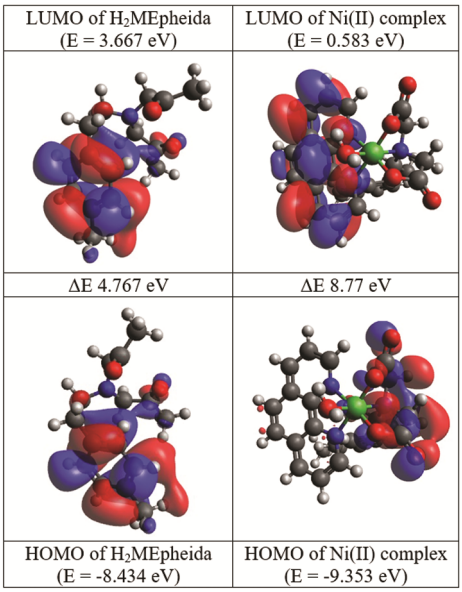

Fig. 5 — The FMOs diagram of H_2MEpheida (up & down) left; and right, up and down the FMOs diagram shown for nickel(II) complex.

found for H_2MEpheida (*Ia*, 3.667 eV) and lowest for Ni(II) complex (*Ia*, 0.583 eV). The Ni(II)-ligand bond lengths and angles measured from computation calculations, slightly differ than that of X-ray data

Table 6 — Calculations of hardness η (in eV), softness σ (in eV^{-1}), dipole moment μ (in D) and thermodynamic parameters of ligands and nickel(II) complex.

Compd	Hardness (η, eV)	Softness (σ, eV^{-1})	Dipole moment (μ, D)
H_2MEpheida	2.381	0.42	4.414
1,10-phen	3.24	0.31	3.219
Ni(II) complex	4.385	0.23	14.068
Compounds	ΔH(kJ mol^{-1})	–ΔS(JK mol^{-1})	ΔG(kJ mol^{-1})
H_2MEpheida	860.8	162	860.5
1,10-phen	491.9	140	491.6
Ni(II) complex	940.8	186	940.6

(Table 5) most likely due to the fact that the theoretically calculated data obtained in gas phase[20,21]. The value of hardness calculated is highest for nickel(II) complex (η, 4.385 eV) and lowest for H_2MEpheida. In contrast, the value of softness was calculated higher for H_2MEpheida (σ, 0.42 eV^{-1}) than that of nickel(II) complex (σ, 0.23 eV^{-1}) (Table 6). Indeed, the effect of hardness and softness properties over the compounds is inversely proportional to each other[23].

Absorption spectra and vibrational properties of nickel(II) complex

The UV-vis absorption spectrum of Ni(II) complex shows three *d-d* transition bands. The ground state term symbol for d^8 configuration assigned to $^3A_{2g}(F)$ and remains same for weak/strong ligand field. A broad band ν_1 = 9960, ν_2 = 17153 and ν_3 = 28653 cm^{-1}. These bands appeared in the spectrum can be assigned to the corresponding electronic transitions $^3A_{2g}(F) \rightarrow {}^3T_{2g}$, $^3A_{2g}(F) \rightarrow {}^3T_{1g}(F)$ and $^3A_{2g}(F) \rightarrow {}^3T_{1g}(P)$. Moreover, spectrum also shows bands at 11904, 30030 and 38462 cm^{-1} which can be assigned to π→π* intra-ligand electronic transition, L→Ni(II) and Ni(II)→L (L = ligand) charge transfer, respectively. The splitting of highest energy d-d band reflecting distortion in octahedral geometry surrounding Ni(II) ion. The value of ligand field Racah parameters have been calculated (B = 1123.48, β = 0.9 and 10Dq = 11234) suggesting the presence of strong field environment NiN_3O_3 around the metal ion consisting of diimine donor[24]. The higher value of $\Delta_o$suggesting strong Nephelauxetic effect on metal-ligands orbital overlapping and follow the following order of the Nephelauxetic series; ($[Ni(H_2O)_6]^{2+}$, Δ_o= 8500 cm^{-1}) < ($[Ni(NH_3)_6]^{2+}$, Δ_o= 10750 cm^{-1}) < ($[Ni(en)_3]^{2+}$, Δ_o= 11200 cm^{-1}) < ([Ni(MEpheida)(phen)(H_2O)], Δ_o= 11234 cm^{-1}). The vibrational frequencies were measured after getting the optimized geometry for both H_2MEpheida and Ni(II) complex using DFT and def2-SVP def2/J basis set. The output file contains only positive Eigenvalue indicating that the optimized structures were stable. The FTIR spectrum of Ni(II) complex along with DFT measured vibrational spectrum given in Fig. S2 (Supplementary material file), showing comparable spectra. The important peaks associated with chromophores can be easily assigned. A broad band 3500-3300 cm^{-1} (depth 3418 cm^{-1}) is due to the ν(O–H) of coordinated and non-coordinated water molecules. Their deformation mode δ(H_2O) can be observed at 1516 cm^{-1}. A very strong peak can be observed at 1600 cm^{-1} for carbonyl group. Two consecutive peaks ν_{as} and $\nu_s(COO^-)$, mode for ionic carboxylate can be seen at 1425 and 1402 cm^{-1} respectively. Some overlapped peaks at ~1800 are due to the presence of aromatic ring and azomethine (C=N) group. Spectrum also show the peaks at 644 and 528 cm^{-1} due to ν (Ni(II)–O) and ν(Ni(II)–N), respectively[25]. The thermodynamic parameters also were measured for the ligands and Ni(II) complex at the same level of theory and the results were listed in Table 6.

Calculation of optical bandgap energy (E_g) for H_2MEpheida ligand and their Ni(II) metal complex

The photovoltaic properties of ligand and nickel(II) complex were calculated through TDDFT absorption data using Tauc's equation, $\alpha h\nu = A(h\nu - E_g)^r$, where r = ½ for indirect and 2 for direct electronic transitions and A = energy independent constant[26,27]. To calculate the bandgap energy (E_g), straight-line plots archived between photon energy E (eV), x axis *versus* $(\alpha h\nu)^{1/2}$ (eV $cm^{-1})^{1/2}$, y axis, for indirect and E (eV), x axis *versus* $(\alpha h\nu)^2$ (eV $cm^{-1})^2$, y axis, for indirect and direct electronic transitions, respectively. The indirect and direct bandgap energy for H_2MEpheida were observed as 4.87 eV and 4.9 eV, respectively (see supplementary file), indicating their insulating in nature. Noteworthy, the direct and indirect electronic transition bandgap calculated for Ni(II) complex 3.97 and 3.76 eV, respectively (Fig. 6). The lower bandgap energy (E_g) values are similar to other reported nickel(II) complexes and reflecting their semi-conductive in nature[28-30].

Thermogravimetric (TGA) analysis of nickel(II) complex

The thermal decomposition of nickel(II) complex was performed using Thermobalance coupled with

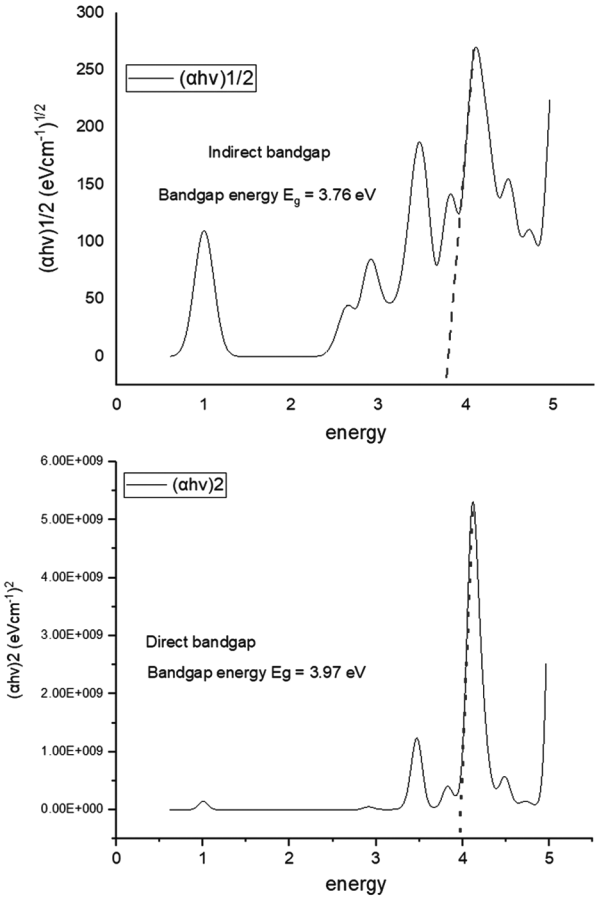

Fig. 6 — Top, indirect and bottom direct bandgap of Ni(II) complex

FT-IR spectrometer in order to identify a series of 25-28 FT-IR spectra of the evolved gases (see supplementary material file for details). The supplementary material file Fig. (S6-A, S6-B) show the% of weight loss of the complex with increase of temperature. The Ni(II) complex decomposes in three steps to give a residue of NiO at ~ 500ºC (calc. 15.638%, exp. 15.643%). The first step started in air-dry flow (55-110ºC) to lose crystalline water molecules to give an averaged formula Ni(MEpheida)(phen) (H_2O).0H_2O. The aqua lose occurs at ~ 140ºC. The second step (300-340ºC) weight loss (calc. 8.410%, exp. 8.419%) was due to the pyrolysis of coordinated arm (–CH_2COO) of MEpheida ligand which yields CO_2, CO and H_2O gases. In third step (350 to 490ºC), major fragment which include aromatic rings of both ligands raptured (calc. 70.749%, exp. 70.958%) to give variety of nitrogenous gases (N_2O, NO_2, NO) along with CO_2, CO, H_2O and traces of CH_4 (Fig. 7)[18].

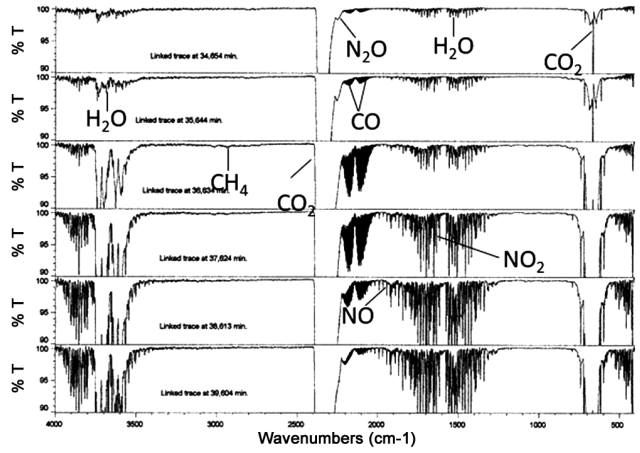

Fig. 7 — FTIR spectra from six steps of the thermo-gravimetric analysis of Ni(II) complex. Spectrum at t = 36.634 min shows traces of methane. In all steps evolving of H_2O, CO, CO_2, N_2O, NO, and NO_2 were observed.

Conclusions

The tri-hydrated Ni(II) complex [Ni(MEpheida)(phen)(H_2O)]·3H_2O, exhibits molecular structure with distorted octahedral geometry of the type 1+2+2+1 around the nickel(II) centre. The IDA arm of MEpheida ligand adopted *fac*-NO_2 conformation. The weak ring-ring intramolecular π,π-interaction between phen and benzene ring of MEpheida affects the crystal pattern of the complex. Our crystallographic information reveals that the centrosymmetric unit cell consists of two asymmetric molecules recognize to each other through ring-ring, π···π-stacking inter-molecular interaction between rings of 1,10-phen. Moreover, due to the presence of diimine donor Nephelauxetic effect follow order of ($[Ni(H_2O)_6]^{2+}$, Δ_o= 8500 cm^{-1}) < ($[Ni(NH_3)_6]^{2+}$, Δ_o= 10750 cm^{-1}) < ($[Ni(en)_3]^{2+}$, Δ_o= 11200 cm^{-1}) < ([Ni(MEpheida)(phen)(H_2O)], Δ_o= 11234 cm^{-1}). Noteworthy, the direct and indirect electronic transition energy bandgap (E_g) calculated for Ni(II) complex is 3.97 and 3.76 eV, respectively. The lower bandgap energy values reflecting their semi-conducting nature.

Acknowledgements

Financial support of Junta de Andalucía (FQM-283 Research Group) and Factoría de Cristalización are acknowledged. Dheerendra Kumar Patel thanks to Spanish Agency for International Cooperation and Development (AECID) for a research grant and University of Granada for his stay at Prof Juan Niclós-Gutiérrez research group.

Supplementary Information

Supplementary information is available in the website http://nopr.niscpr.res.in/handle/123456789/58776.

References

1 Sanchez-Moreno M J, Choquesillo-Lazarte D, González-Pérez J M, Carballo R, Martin-Ramos J D, Castiñeiras A & Niclós-Gutiérrez J, *Polyhedron*, 22 (2003) 1039.

2 Patel D K, Choquesillo-Lazarte D, González-Pérez J M, Domínguez-Martín A, Matilla-Hernandez A, Castiñeiras A & Niclós-Gutiérrez J, *Polyhedron*, 29 (2010) 683.

3 Patel D K, Choquesillo-Lazarte D, Domínguez-Martín A, González-Pérez J M & Niclós-Gutiérrez J, *Indian J Chem*, 60A (2021) 806.

4 Patel D K, Dominguez-Martin A, Brandi-Blanco M P, Choquesillo-Lazarte D, Nurchi V M & Niclós-Gutiérrez J, *Coord Chem Rev*, 256 (2012)193.

5 Patel D K, Dominguez-Martin A, Choquesillo-Lazarte D, González-Pérez J M & Niclós-Gutiérrez J, *J Coord Chem*,75 (2022) 2814.

6 Bugella-Altamirano E, Choquesillo-Lazarte D, González-Pérez J M, Sánchez-Moreno M J, Marín-Sánchez R, Martín-Ramos J D, Covelo B, Carballo R, Castiñeiras A& Niclós-Gutiérrez J, *Inorg Chim Acta*, 339 (2002) 160.

7 Bruker, *APEX2 Software, Bruker AXS Inc*. V2008.1, Madison, Wisconsin, USA, (2008).

8 Sheldrick G M, SADABS, Program for Empirical Absorption Correction of Area Detector Data, University of Göttingen, Germany, (2001).

9 Sheldrick G M, *Acta Crystallogr, A*71 (2015)3.

10 Sheldrick G M, *SHELXL-97, Program for the Refinement of Crystal Structures*, (University of Göttingen, Germany) 1997.

11 Spek A L, PLATON, *A Multipurpose Crystallographic Tool*, (Utrecht University, Utrecht, The Netherlands) 2003.

12 Macrae C F, Bruno I J, Chisholm J A, Edgington P R, McCabe P, Pidcock E, Rodríguez-Monge L, Taylor R, van de Streek J & Wood P A, *J Appl Cryst*, 41 (2008) 466.

13 Neese F, *The ORCA program system*, (Wiley Interdiscip Rev) 2012.

14 Becke A D, *Phys Rev A*, 38 (1988) 3098.

15 Becke A D, *J Chem Phys*, 98 (1993) 1372.

16 Lee C, Yang W & Parr R G, *Phys Rev B*, 37 (1988) 785.

17 Benhamed K, Boukli-Hacene L & Harek Y, *Mediterr J Chem*, 4 (2015) 209.

18 Bugella-Altamirano E, González-Pérez J M, Sicilia Zafra A G, Niclós-Gutiérrez J & Castiñeiras-Campos A, *Polyhedron*, 19 (2000) 2463.

19 Ricca A &Bauschlicher C W, *J Phys Chem*, 99 (1995) 9003.

20 Scottt A P & Radom L, *J Phys Chem*, 100 (1996) 16502.

21 Petersson G A & Al-Laham M A, *J Chem Phys*, 94 (1991) 6081.

22 Weigend F & Ahlrichs R, *Phys Chem Chem Phys*, 7 (2005) 3297.

23 Weigend F, *Phys Chem Chem Phys*, 8 (2006) 1057.

24 Sánchez-Moreno M J, Choquesillo-Lazarte D, González-Pérez J M, Carballo R, Martín-Ramos J D, CastiñeirasA &Niclós-Gutiérrez J, *Polyhedron*, 22(2003) 1039.

25 Hosny N M & Sherif Y E, *Spectrochim ActaPart B*, 136 (2015) 510.

26 Tauc J, Grigorovici R &Vancu A, *Basic Solid-State Phys*, 15 (1966) 627.

27 Abdel-Rhman M H, Hussien M A, Mahmoud H M & Hosny N M, *J Mol Struc*, 1196 (2019) 417.

28 Abdel-Rhman M H, Motawea R, Belal A & Hosny N M, *J Mol Struc*, 1251 (2022) 131960.

29 Hosny N M, Hussien M A, Motawa R, Belal A & Abdel-Rhman M H, *App Organomet Chem*, 34 (2020) 5922.

30 Hosny N M, Sayed El, Morsy A El & Sherif Y E, *J Rare Earths,* 33 (2015) 758.